

# PRECIPITATION AND TEMPERATURE VARIABILITY OVER SOUTH AMERICA FROM 1860 TO 2100

Simone Erotildes Teleginski Ferraz<sup>1</sup>, Tércio Ambrizzi<sup>2</sup>, Rosmeri Porfirio da Rocha<sup>2</sup>,  
Santiago Vianna Cuadra<sup>2</sup>

<sup>(1)</sup>Departamento de Física - Universidade Federal de Santa Maria - Brasil

<sup>(2)</sup>Departamento de Ciências Atmosféricas - Universidade de São Paulo - Brasil

## Introduction

A complex variety of regional and remote factors contribute to define the climate of South America. The continental mass extends across the equator from about 10°N to 55° S and has unique geographical features. The high and sharp Andes Mountains rise along the Pacific coast on the west. Surface conditions include the world's largest rain forest in Amazonia and driest Desert in Atacama in northern Chile, as well as a high desert in the Altiplano. Climate variability elsewhere significantly impacts the climate over South America. Links between sea surface temperature (SST) anomalies associated with El Niño/Southern Oscillation (ENSO) and rainfall as well as circulation anomalies over the continent have been demonstrated. In turn, climate variability over South America can influence atmospheric patterns in the surrounding oceans and beyond. The climate of South America is a topic of investigation that is

scientifically exciting and of extraordinary relevance to the millions who live on the continent (Paegle et. al, 2002).

In austral summer, as the major heating zone migrates to the subtropics, a thermal low-pressure system develops over the Chaco region, in central South America. The low pressure system over northern Argentina and western Paraguay is a climatological feature present throughout the year, but strongest during the summer. Anomalous cross equatorial flow penetrates the continent, carrying moisture. The flow becomes northwesterly, is channeled southward by the Andes mountains, and turns clockwise around the Chaco low. Low-level wind and moisture convergence associated with the interaction of the continental low with the South Atlantic high and the northeasterly trade winds result in enhanced precipitation in the Amazon, and Central and Southeast Brazil (Lenters and Cook, 1995). The southeastward extension of cloudiness and

precipitation towards the Atlantic Ocean is referred to as South Atlantic Convergence Zone (SACZ) (Kodama 1993,a,b). During the SACZ most active stage (DJF), the upper level anticyclonic center moves southward from the Amazon, setting up the “Bolivian High”. East of this high and over the Atlantic Ocean close to the coast of Northeast Brazil, there is a upper lever cyclone known as the “Nordeste trough” (Virji 1981; Kousky and Ropelewski 1997).

Summer precipitation in South America undergoes variability in several time-scales. The spatial distribution of the contribution from the synoptic and intraseasonal variability in the summer (December through February) precipitation is discussed here. For this study, we used 240 years of precipitation and temperature data from 1860 to 2100. Preliminary results will be presented below.

## **Data and Methodology**

For this study, British Atmospheric Data Centre (BADC) precipitation and 2m air temperature data are used. This dataset contains output data from a number of models from the Hadley Centre (at the UK Met office) in a friendly format generated by the Climate Impact community project. The Climate Impacts LINK Project is funded by the UK Department of the Environment, Food and Rural Affairs (DEFRA), (<http://badc.nerc.ac.uk>).

This data has a resolution of 2.5° (latitude) x 3.75° (longitude), producing a global grid of 96 x 73 grid cells, with a equivalent resolution of 417 km x 278 km at the Equator, reducing to 295 km x 278 km at 45° of latitude (comparable to a spectral resolution of T42). Furthermore, this data has 360 days (monthly with 30 days) and it is available from 1860 to 2100.

To obtain the intraseasonal and synoptic signals, precipitation and temperature data were filtered using a Lanczos filter to retain periods in the ranges of 10-100 and 2-10 days.

The principal component analysis was performed on the intraseasonal and synoptic data for December to February in the periods 1860-1890, 1870-1900, 1880-1910, ..., 2070-2100 years (30 years moving means).

Power spectra of factor scores are computed for 2700 days mean series beginning at 1<sup>st</sup> December to 30 February. At each factor loading of interest, spectra are calculated for individual periods and these are then averaged.

## **Preliminary Results**

### **Variability patterns**

The principal component analyses from the intraseasonal precipitation time series have 22 groups. From the analysis of the first mode, which has the larger variance, two distinct patterns were found

among the groups. The first one appears in the following years: 1880-1900, 1890-1910, 1900-1930, 1910-1940, 1970-2000, 1980-2010, 1990-2020, 2020-2050, 2030-2060, 2040-2070, 2050-2080 e 2060-2090 and it

will be called as a simple mode (Fig.1). The spectral density from each PC time series is shown in Fig.2. In this figure, the black line indicates the average of the all spectra.

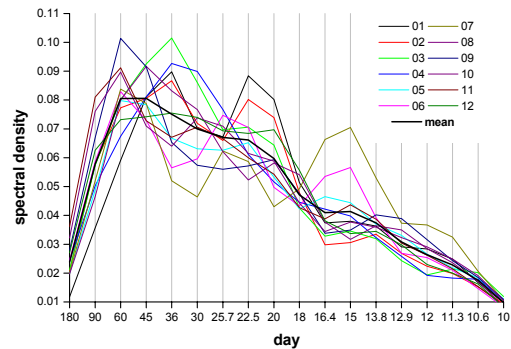
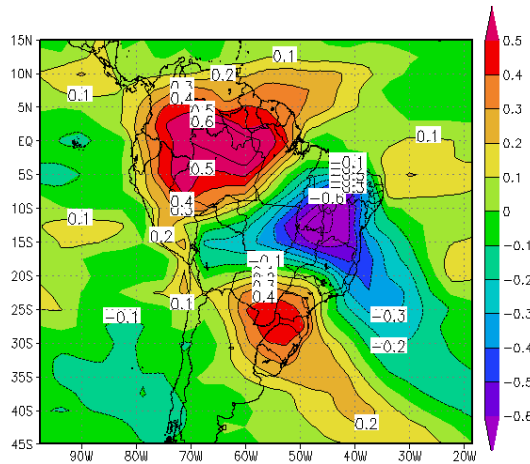


Figura 1: 1° mode of the intraseasonal band: Simple mode.

Figura 2 – Spectral density of the principal components for each one of the simple mode series. The black line indicates the average spectrum.

The second pattern which will be called complex mode is evident among the following years group: 1860-1890, 1870-1910, 1940-1970, 1950-1980, 1960-1990, 2000-2030 e 2010-2040, and it is presented in the Fig.3. Fig.4 shows the spectral density for each one of the PC components (factor scores).

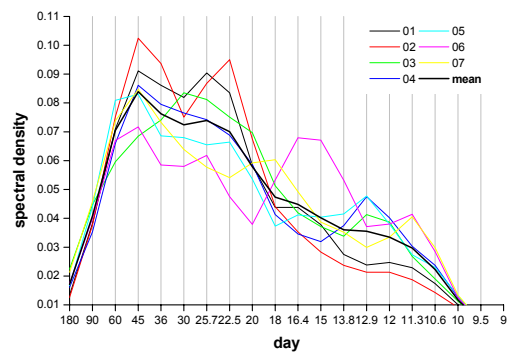
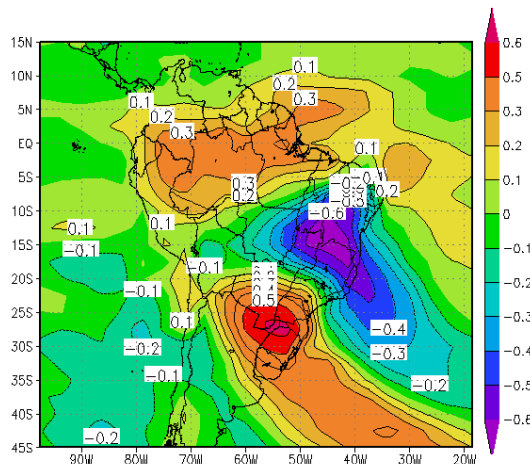


Figura 3: 1° mode of the intraseasonal band: Complex mode.

Figura 4 – Spectral density of the principal components for each one of the complex mode series. The black line indicates the average spectrum..

The simple mode shows larger variability over the continent and it has two cores with opposite signals, one on the Northeast Brazil and another over in the Southern Brazil (Fig.1). A third distinct core also stands out in the Northern part of the South American continent, having the same signal of the south part. On the other hand, the complex mode (Fig.3) still shows the opposite pattern between the northeast and south of Brazil but values larger over the Atlantic Ocean. Also, the northern core seems weaker and less significant in this case.

The simple mode mean spectral density (black line in Fig.2) peaks at 60 and 22 days while the complex mode shows maxima at 45 and 25 days. This result suggests that the modes may have different origins. Besides, when extreme precipitation events were calculated for these modes ( $\pm 1.4$  standard deviation) the simple mode presented less positive and negative events than the complex mode. Also, analyzing the periods used for each mode, it seems that a decadal variability is modulating the intraseasonal precipitation. However further analysis is still necessary to verify this hypothesis.

The principal component analyses from the synoptic precipitation time series also have 22 groups being similar to the intraseasonal PC ones. From the analysis of the first mode, which shows the highest variance (Fig.5), one can see that there is one strong positive core flanked by negative ones. The poleward pattern is located over the region well known as cyclogenetic (Gan and Kousky 1981), being also the preferential path of the cold fronts. The strong positive core is over the southern Bolivia, northern Argentina and extends toward the Atlantic Ocean through the Southern Brazil. In fact this mode pattern may represent the region of the main position of the South American Low Level Jet (e.g. Marengo et al 2004) which is responsible for bring moisture and warm air from the Amazon region. The equatorward pattern is located around the South Atlantic Convective Zone main position (e.g. Jones and Carvalho, 2002) and it is probable related to this summer atmospheric system. The spectral density of the synoptic PC series (Fig.6) shows a peak at 8 days which is coherent with the synoptic time scale of the mode.

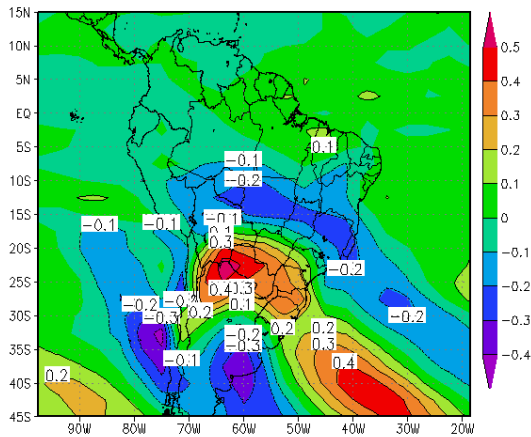


Figure 5 : 1° mode of the synoptic band

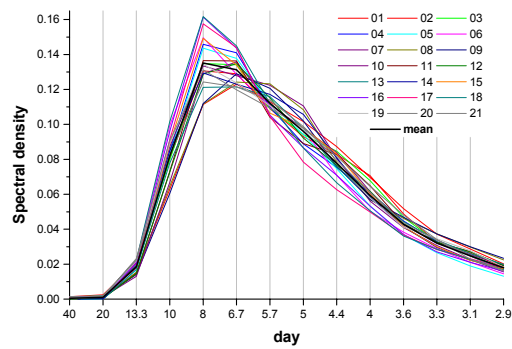


Figure 6 – As Fig.2 but for the synoptic mode.

Principal Component analysis for intrasazonal and synoptic temperature series was also carried out. The first mode shows two distinct patterns among the 22 groups used. The pattern one appeared in the following year periods: 1860-1890, 1880-1910, 1910-1940, 1920-1950, 1930-1960, 1940-1970, 2040-2070 and it will be called AS mode (Fig.7). The second pattern (to be referred as SAS mode) was present in the other year's group (Fig.9).

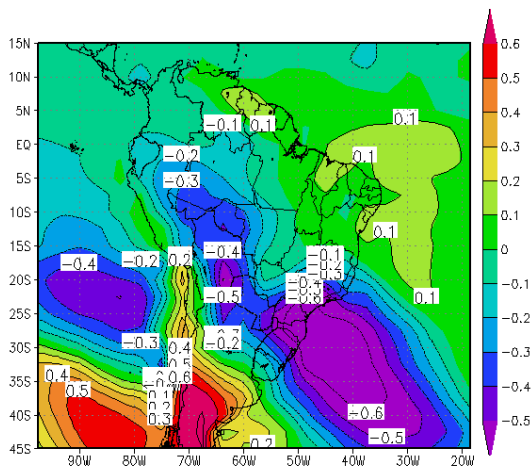


Figure 7 : As in Fig.1 but for the temperature of the mode AS

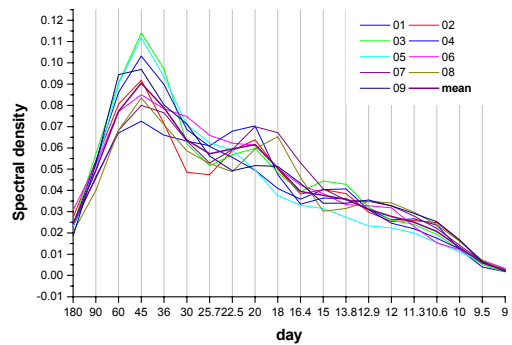


Figure 8– As in Fig.2 but for the mode AS of the temperature.

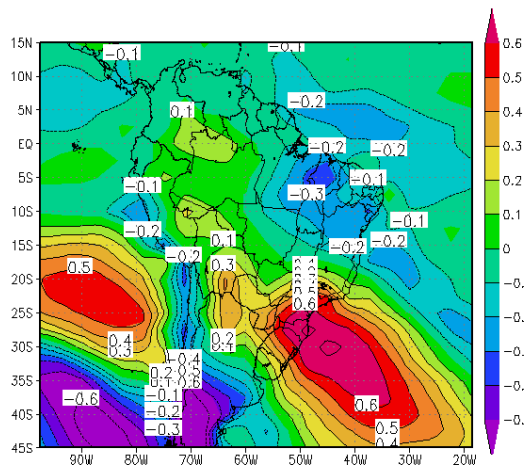


Figure 9 : As in Fig.1 but for the SAS mode of temperature.

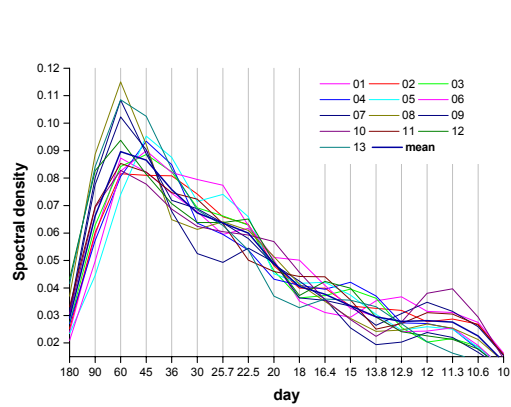


Figure 10– As in Fig.2 for the SAS mode of temperature.

The pattern of the AS mode presents a strong signal over the south and center-west of Brazil (Fig.7). However, the core of the SAS mode is more intense and concentrated to the south of Brazil. This pattern suggests a temperature change in the region from the mid of the last century since the mode AS data is from the 1980's up to 1950's. The spectrum density shows peaks at 45 and 20 days for the AS mode (Fig.8) and around 60 days for the SAS (Fig.10).

On the synoptic band, it is only found one pattern for the first mode (Fig.11). As it would be expected its spectrum (Fig.12) presents a peak around day 8, similar to the precipitation analysis (Fig.6).

The temperature variability in the synoptic band seems to be significant in the south of the South America only, where it shows positive and negative signals in the region.

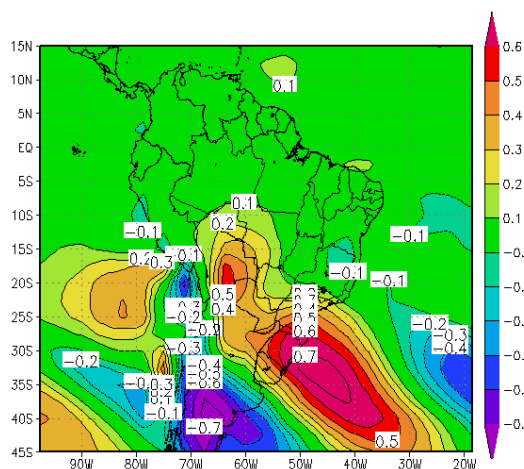


Figure 11 : As in Fig.5 but for the temperature mode.

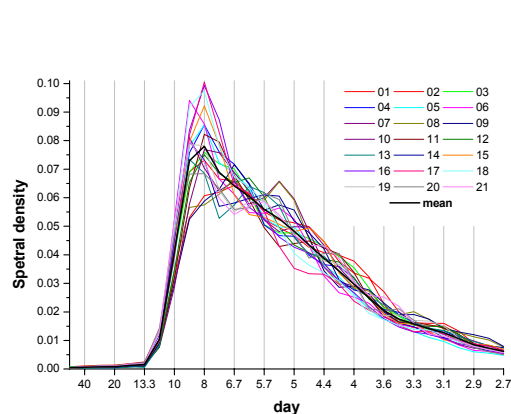


Figure 12 : As in Fig.6 but for the temperature mode.

## Final comments

The Principal component analysis from the control integration of the Hadley Centre model for the intraseasonal band showed two distinct patterns for two data sets from different years. The analyzes of these two data sets suggested a possible decadal variability. From the temperature analysis it was noticed that there seems to be a change in the temperature pattern in the middle of the 20<sup>th</sup> century.

The results presented here are still preliminaries. There is the need to further investigate the interannual and inter-decal variability modes in order to understand how they will be changed in an atmosphere with double CO<sub>2</sub> as predicted by the Global Circulation Models nowadays.

## Acknowledgments

This work is part of the "PROBIO" project funded by the MMA/BIRD/GEF/CNPq and the Global Opportunity Fund-GOF from United Kingdom. We are grateful to the British Atmospheric Data Centre which provided us with access to the Met Office Land Surface Observation Stations Data. One of us (TA) was also partially funded by CNPq, FAPESP and IAI – CRN055. We are grateful to the British Atmospheric Data

Centre which provided us with access to the Met Office Land Surface Observation Stations Data.

## Bibliography:

JONES, C.; CARVALHO, L.M. V., 2002, Active and Break Phases in the South American Monsoon System , **Journal of Climate**, Volume: 15, Pages: 905-914

KOUSKY, V. E.; ROPELEWSKI, C. F., 1997, Tropospheric Seasonally Varying Mean Climate over the Western Hemisphere (1979-1995) , **NASA** no. 19980015167

KOUSKY, V. E.; GAN, M. A., 1981, Upper tropospheric cyclonic vortices in the tropical South Atlantic ,

**Tellus**. Vol. 33, pp. 538-551. Dec. 1981

KODAMA Y. M. Large scale common features of sub-tropical convergence zones (the Baiu frontal zone, the SPCZ, and the SACZ). Part I: Characteristics of subtropical frontal zones. **Journal of the Meteorological Society of Japan**, v. 70, p. 813 – 836, 1993.

KODAMA Y. M. Large scale common features of sub-tropical convergence zones (the Baiu frontal zone, the SPCZ, and the SACZ). Part II: Conditions of the circulations for generating the STCZs. **Journal of the Meteorological Society of Japan**, v. 70, p. 581 – 610, 1993.

LENTERS , J.D.; COOK, K.H. 1995, Simulation and Diagnosis of the Regional Summertime Precipitation Climatology of South America, **Journal of Climate**: Vol. 8, No. 12, pp. 2988–3005.

MARENGO J. A., 2004, Interdecadal variability and trends of rainfall across the Amazon basin, **Theoretical and Applied Climatology** , Volume 78, pg. 79-96.

PAEGLE, J.N., MO, K. C., 2002, Linkages between Summer Rainfall Variability over South America and Sea Surface Temperature Anomalies, **Journal of Climate**, v15,pag.1389-1407

VIRJI, H., 1981, A Preliminary Study of Summertime Tropospheric Circulation Patterns over South America Estimated from Cloud Winds, **Monthly Weather Review**: Vol. 109, No. 3, pp. 599–610.